



Brain Function Network and Young Adult Smokers: A Graph Theory Analysis Study

Ying Tan¹, Jing Chen², Weiwei Liao^{1*} and Zhaoxin Qian^{3*}

¹ Health Management Center, Xiangya Hospital, Central South University, Changsha, China, ² Center of Stomatology, Xiangya Hospital, Central South University, Changsha, China, ³ Department of Emergency, Xiangya Hospital, Central South University, Changsha, China

OPEN ACCESS

Edited by:

Qinghua He,
Southwest University, China

Reviewed by:

Dahua Yu,
Inner Mongolia University of Science
and Technology, China
Kai Yuan,
Xidian University, China

*Correspondence:

Weiwei Liao
1532950695@qq.com
Zhaoxin Qian
xyqzx@csu.edu.cn

Specialty section:

This article was submitted to
Psychopathology,
a section of the journal
Frontiers in Psychiatry

Received: 15 May 2019

Accepted: 25 July 2019

Published: 30 August 2019

Citation:

Tan Y, Chen J, Liao W and Qian Z
(2019) Brain Function Network and
Young Adult Smokers: A Graph
Theory Analysis Study.
Front. Psychiatry 10:590.
doi: 10.3389/fpsy.2019.00590

Cigarette smoking is associated with abnormalities in the widespread inter-regional functional connectivity of the brain. However, few studies focused on the abnormalities in the topological organization of brain functional networks in young smokers. In the current study, resting-state functional magnetic resonance images were acquired from 30 young male smokers and 32 age-, gender-, and education-matched healthy male nonsmokers. A functional network was constructed by calculating the Pearson correlation coefficients among 246 subregions in the human Brainnetome Atlas. The topological parameters were compared between smokers and nonsmokers. The results showed that the functional network of both young smokers and nonsmokers had small-world topology. Compared to nonsmokers, young smokers exhibited a decreased clustering coefficient (C_p) and local network efficiency (E_{local}). C_p and E_{local} were negatively correlated with the duration of cigarette use. In addition, increased nodal efficiency (E_{nodal}) was mainly located in the prefrontal cortex (PFC), cingulate gyrus, insula, and caudate. Decreased connectivities among the PFC, cingulate gyrus, insula, basal ganglia (of specific node), and thalamus were also observed. In sum, we revealed the abnormal topological organization of brain functional networks in young smokers, which may improve our understanding of the neural mechanism of young smokers from a brain functional network topological organization perspective.

Keywords: young smokers, brain functional networks, graph theory analysis, resting-state functional magnetic resonance imaging, topological organization

INTRODUCTION

Cigarette smoking is associated with serious health problems, such as brain-, heart-, and lung-related diseases (1). The majority of lifelong smokers and those with higher levels of nicotine dependence are people who started smoking at an early age (2–5). Structural and functional deficits have been found in the brains of young smokers (6–9). The abnormal cortical thickness and gray matter volume/density mainly in the frontal cortex, anterior cingulate cortex, and striatum have been detected in young smokers (6, 10, 11). In addition, the resting-state functional connectivity (RSFC) among the dorsolateral prefrontal cortex (PFC), orbitofrontal cortex (OFC), and striatum were significantly reduced in smokers (6, 12, 13). These regional and circuit-level structural and functional abnormalities in young smokers (13–15) may contribute to whole-brain functional network changes. Thus, the main purpose of the current study is to detect the changes in the topological organization of brain functional networks in young smokers.

Modeling the human brain as a complex network has provided a powerful mathematical framework to characterize the functional architecture of the brain (16). Graph theory analysis (GTA) provides a powerful mathematical framework for characterizing the intrinsic topological organization in the whole-brain functional networks, such as the small-world property, connectivity, global efficiency (E_{global}), and E_{nodal} (16–18). The small-world network is characterized by a distinctive combination of high clustering coefficient (C_p) and short characteristic path length (L_p), which can quantify efficient information segregation and integration and may facilitate the spread of information in networks (19). The brain functional network's efficiency can be quantitatively calculated by GTA and characterize the capacity for parallel information transfer at the brain node and global levels (20). GTA has been applied to the study of brain-related diseases in both brain structural and functional networks in addiction research (18, 21–24). Less efficient network architecture and disruptions in the topological organization of brain networks had been observed in smokers (25). Similarly, heroin-dependent patients showed decrease normalized C_p (γ) and small-worldness in the brain functional networks compared to health controls (22). GTA has provided novel insights into the neurobiological mechanisms for young smokers. Clear evidence showed that the number of parcellations will impact the local characteristics and metrics of the brain network architecture. As the number of nodes increased, an increased stability of network metrics could be observed (26). Previous studies constructed the structural and functional networks with 90 regions of interest from the Automated Anatomical Labeling template as network nodes (21–24, 27). To increase the accuracy of the brain function network analysis based on GTA, in the current study, we employed 246 regions in the human Brainnetome Atlas—a detailed fine-grained, cross-validated atlas that contains information on both anatomical connectivity and FC patterns—to parcellate gray matter into distinct regions (28).

Therefore, in this study, we aimed to compare the differences in topological organization of brain functional networks (246 regions) between nonsmokers and young smokers. Based on previous addiction findings on brain functional network topography, we hypothesized that (1) differences in the global and node topological parameters should be detected between nonsmokers and young smokers; (2) compared to nonsmokers, young smokers showed significant FC among the nodes in the PFC, striatum, and insula; and (3) abnormal topological properties of the brain functional network may be related to smoking behaviors in young smokers. We hoped that our findings could improve our understanding of the neurobiological mechanisms by revealing the brain functional network organization in young smokers.

MATERIALS AND METHODS

All procedures of the present study were approved by the Medical Ethical Committee of the Xiangya Hospital of Central South University. All participants and their parents gave written informed consent after the experimental procedure was fully explained.

Participants

Thirty young male smokers (mean age, 21.2 ± 1.15 years) and 32 matched healthy male nonsmokers (mean age, 20.8 ± 1.08 years) were recruited from local universities (Table 1). In the current study, all young smokers met the diagnostic criteria of nicotine dependence in the Diagnostic and Statistical Manual of Mental Disorders, Fifth Edition, and have not abstained from smoking for longer than 3 months since they had started smoking. The nicotine dependence level of young smokers was assessed by the Fagerström Test for Nicotine Dependence (FTND). The cumulative amount of nicotine intake was indexed by pack-year. Nonsmokers were recruited from people who smoked no more than five cigarettes in their lifetime. None of the subjects have physical illness (brain tumor, obstructive lung disease, hepatitis, or epilepsy), neurological disease (e.g. stroke), or claustrophobia according to clinical evaluations and medical records. None of the subjects reported daily consumption of alcohol, drug abuse, or dependence (other than nicotine dependence for young smokers) or current medication use that may affect cognitive functioning. The carbon dioxide level in expired air, as measured by the Smokerlyzer system (Bedfont Scientific Ltd., Rochester, UK), was verified as 3 ppm in nonsmokers and ≤ 8 ppm in the abstinence state, showing a distinct reduction for young smokers compared to those not currently smoking.

Image Acquisition

This experiment was carried out on a 3 T magnetic resonance imaging (MRI) system (Signa; General Electric) with an eight-channel phase-array head coil at Xiangya Hospital of Central South University. Participants were asked to refrain from smoking for 60 min immediately preceding the scan. All the subject's heads were positioned carefully with comfortable support, and earplugs were used to reduce scanner noise. The resting-state functional images were obtained with the following parameters: 30 contiguous slices with a slice thickness of 5 mm; repetition time = 2,000 ms; echo time = 30 ms; flip angle = 90° ; field of view = 240×240 mm²; data matrix = 64×64 ; and total volumes = 180. During the entire scan, subjects were instructed to keep their eyes closed, relax their minds, but not fall asleep and remain as motionless as possible.

Data Preprocessing

Statistical Parametric Mapping software (SPM8; <http://www.fil.ion.ucl.ac.uk/spm>) was used to perform data preprocessing.

TABLE 1 | Demographic characteristics of nonsmokers and young smokers in this study.

Items	Smokers (<i>n</i> = 30)	Controls (<i>n</i> = 32)	<i>t</i>	<i>p</i>
Age (years)	21.2 ± 1.15	20.8 ± 1.08	-1.254	0.215
Levels of education (years)	14.07 ± 0.58	14.09 ± 0.53	0.191	0.849
CPD	15.6 ± 5.10	—	—	—
Age at smoking onset	15.7 ± 2.50	—	—	—
Years of smoking	4.5 ± 2.47	—	—	—
Pack-years	3.7 ± 2.95	—	—	—
FTND	4.8 ± 1.66	—	—	—

Data preprocessing included the following steps. First, the initial 10 volumes were discarded for magnetization equilibration for each dataset. Second, slice-timing correction and head-motion correction were performed in the remaining volumes to exclude the subjects with a maximum displacement greater than 1.5 mm or head rotation greater than 1.5° . Third, corrected images were normalized to the Montreal Neurological Institute space and resampled to a 3 mm isotropic voxel. The nuisance signal regression was carried out by including the six motion parameters, their first-order temporal derivatives, white matter, and ventricular cerebrospinal fluid signal (14-parameter regression). Finally, a temporal band-pass filter (0.01–0.08 Hz) was applied to reduce the effects of high-frequency physiological noises.

Brain Functional Network Construction

Network Node Definition

To define the nodes of the network, we chose 246 regions (210 cortical and 36 subcortical subregions) for whole-brain parcellation, providing a fine-grained, cross-validated atlas and containing information on both anatomical and functional connections (28). Each brain region represented a node of the functional network. This set of 246 putative functional regions was shown to more accurately represent the information present in the network relative to voxel-wise and atlas-based parcellation approaches (29). The detailed information can be found <http://atlas.brainnetome.org/>.

Network Edge Definition

To determine the edges of the network, the regional mean time series of all possible pairs of 246 brain regions were evaluated for Pearson correlation coefficients and z -transformed correlation coefficients to generate 246×246 whole-brain FC matrices for each subject. Then, the absolute z correlation matrices were thresholded to obtain binarized matrices [i.e., adjacency matrices $A = (a_{ij})$] according to a threshold range of $0.10 < \text{cost} < 0.40$ with intervals of 0.01 (25) to avoid correlation-level differences between groups (30). Cost was defined as the ratio of the existing number of edges to the maximum possible number of edges in a network. The entry a_{ij} was 1 when the absolute z -value between regions i and j exceeded the threshold and 0 otherwise.

Network Analysis

The topological properties of the brain functional networks were explored for each threshold, including small-world parameters [γ , normalized characteristic path length (λ), and scalar small-worldness (σ)], network efficiency [global level: global network efficiency (E_{global}) and local network efficiency (E_{local}); regional level: E_{nodal} for each node i as a nodal metric], and global parameters (area under the curve for each network measure, which provides a summarized scalar for topological properties).

Small-World Parameters

C_p and L_p are two important elements of small-world network parameters that were first proposed by Watts and Strogatz (31).

$$C_p = \frac{1}{N} \frac{E_i}{D_i(D_i - 1) / 2},$$

where E_i is the number of existing connections within the network and D_i is the degree of node i . The C_p of a network quantifies the extent of local interconnectivity or cliquishness of the network (31).

$$L_p = \frac{1}{N(N-1)} \sum_{i \neq j \in G} L_{i,j},$$

where $L_{i,j}$ is the L_p between nodes i and j . The characteristic path length of the network (L_p) measures the potential for integration between brain regions (31).

The C_p and L_p of the brain networks were compared to those of random networks to examine the small-world properties. In this study, we defined the normalized L_p (λ), $\lambda = L_p^{\text{real}} / L_p^{\text{rand}}$, and the γ , $\gamma = C_p^{\text{real}} / C_p^{\text{rand}}$. One hundred matched random networks, which had the same number of nodes, edges, and degree distribution as the real networks (32), were generated. L_p^{rand} and C_p^{rand} are the mean C_p values and the mean L_p of 100 matched random networks. When a network meets the criteria of $\gamma > 1$ and $\lambda \approx 1$ (25) or $\delta = \gamma / \lambda > 1$ (33), the network has small-world properties.

Network Efficiency

E_{global} measures the efficiency of parallel information transfer in the network (34):

$$E_{\text{global}} = \frac{1}{N(N-1)} \sum_{i=1}^N \sum_{\substack{j=1 \\ j \neq i}}^N \frac{1}{L_{ij}}.$$

E_{local} quantifies the fault tolerance in the network and reveals the communication efficiency among the immediate neighbors of the node i when it is removed (34):

$$E_{\text{local}} = \frac{1}{N} \sum_{i \in G} E_{\text{global}}(G_i),$$

where G_i denotes the subgraph composed of the nearest neighbors of node i .

Regional Nodal Characteristics

The E_{global} of a node i (E_{nodal}) measures the information propagation ability of a node with the rest of the nodes in the network.

$$E_{\text{nodal}} = \frac{1}{N-1} \sum_{j \neq i \in G} \frac{1}{L_{i,j}},$$

Statistical Analysis

Comparisons of Demographic Variables

The differences in demographic characteristics between 30 young smokers and 43 nonsmokers were tested with the two-sample t test using SPSS 20.0 software.

Comparisons of Global Parameters and Regional Efficiency

We detected the significant differences in network topological properties (C_p , L_p , E_{global} , and E_{local}) and E_{nodal} between nonsmokers and young smokers using nonparametric permutation tests. Specifically, the group differences were obtained using a

two-sample t test with $p = 0.05$. The process for the nonparametric permutation tests was as follows: For each permutation, two sets of data were pooled to create a single set. Then, we selected the actual data of one group from the merged data randomly as the new group, with the rest constituting the other group. Then, the t value was calculated and acted as the statistical magnitude. A total of 5000 permutations were performed to obtain an empirical estimate of the null distribution of the differences. We sorted the 5000 recorded differences and computed the proportion of the between-group differences exceeding the differences in real cortical networks. The threshold for statistical significance was $p < 0.005$. The network-based statistical approach was used to localize the abnormal FC about the specific pairs of brain regions in the WM network. Regression analyses were performed to examine the association of the network parameters with duration cigarette of use, controlling for age and years of education as covariate variables. The results were visualized using the BrainNetViewer package (<http://www.nitrc.org/projects/bnv>).

RESULTS

Demographic Information

All of the participants were right-handed males. There was no difference between nonsmokers and young smokers in the distributions of age ($p = 0.215$) or level of education ($p = 0.849$; **Table 1**). According to self-reports, the number of cigarettes per day (CPD) in 30 young smokers was 15.6 ± 5.1 , the mean FTND score was 4.8 ± 1.66 , the mean pack-years were 3.7 ± 2.95 , and the mean duration of smoking was 4.5 ± 2.47 years.

Efficient Small-World Brain Functional Networks

For nonsmokers and young smokers, their functional networks showed small-world properties in the entire threshold range of $0.10 < \text{cost} < 0.40$ (**Figures 1 and 2**). Across the wide threshold range ($0.10 < \text{cost} < 0.40$), all the subjects exhibited a higher C_p and E_{local} yet had similar L_p and E_{global} compared to 100 random networks (**Figure 1**) (31). In addition, compared to 100 random networks, all the groups had higher γ values (i.e., $\gamma > 1$) and nearly identical normalized L_p (i.e., $\lambda \approx 1$), and the σ of each network was larger than 1.1 ($\delta > 1.1$) for all subjects in the entire threshold range of $0.10 < \text{cost} < 0.40$ (**Figure 2**).

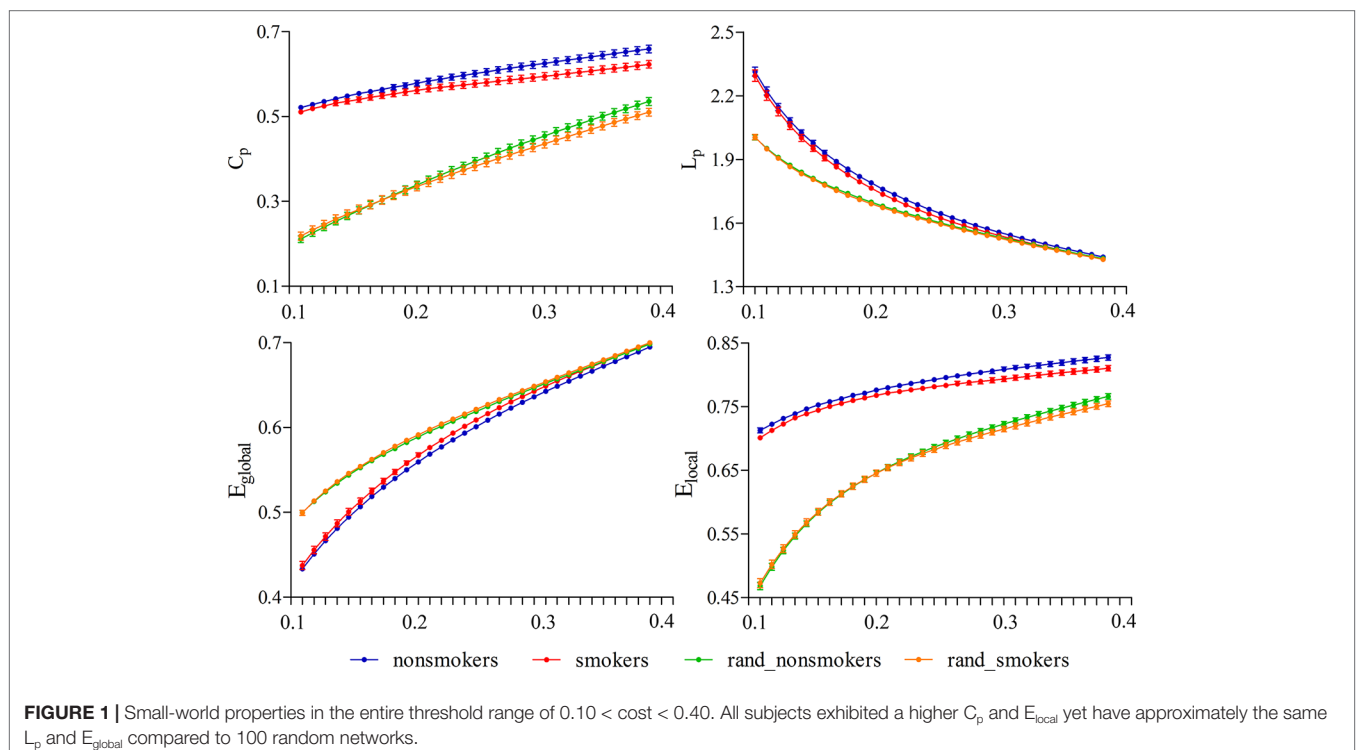
Global Topology of Brain Function Networks

Statistical analysis revealed significant differences in the global parameters between nonsmokers and young smokers (**Figure 3A**). Compared to nonsmokers, young smokers showed a significantly decreased C_p ($p = 0.023$) and E_{local} ($p = 0.0086$) (**Table 2**). C_p ($r = -0.458$; $p = 0.011$) and E_{local} ($r = -0.431$; $p = 0.017$) were negatively correlated with the duration of cigarette use (**Figures 3B, C**).

TABLE 2 | Comparisons of global network measures between nonsmokers and young smokers.

	C_p	L_p	E_{local}	E_{global}
Control	0.1785 (0.011)	0.517 (0.014)	0.235 (0.005)	0.177 (0.004)
Satiety	0.1724 (0.012)	0.511 (0.011)	0.232 (0.005)	0.178 (0.003)
p	0.0232*	0.0596	0.0086*	0.9612

* $p < 0.05$ compared within groups.



Economic small-world topology for health control and young smokers

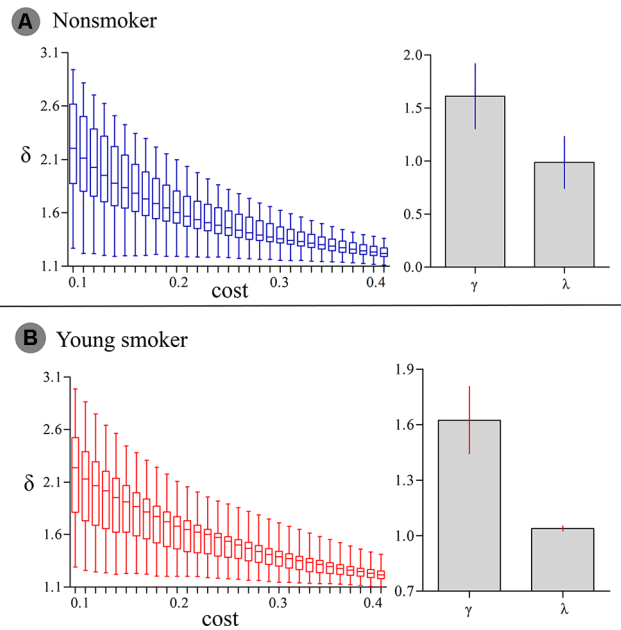


FIGURE 2 | (A) In nonsmokers, the σ of each network was larger than 1.1 ($\delta > 1.1$) in the entire threshold range of $0.10 < \text{cost} < 0.40$. Compared to 100 random networks, all groups had higher γ values (i.e., $\gamma > 1$) and nearly identical normalized L_p (i.e., $\lambda \approx 1$). **(B)** In smokers, similar δ , γ and λ values were detected.

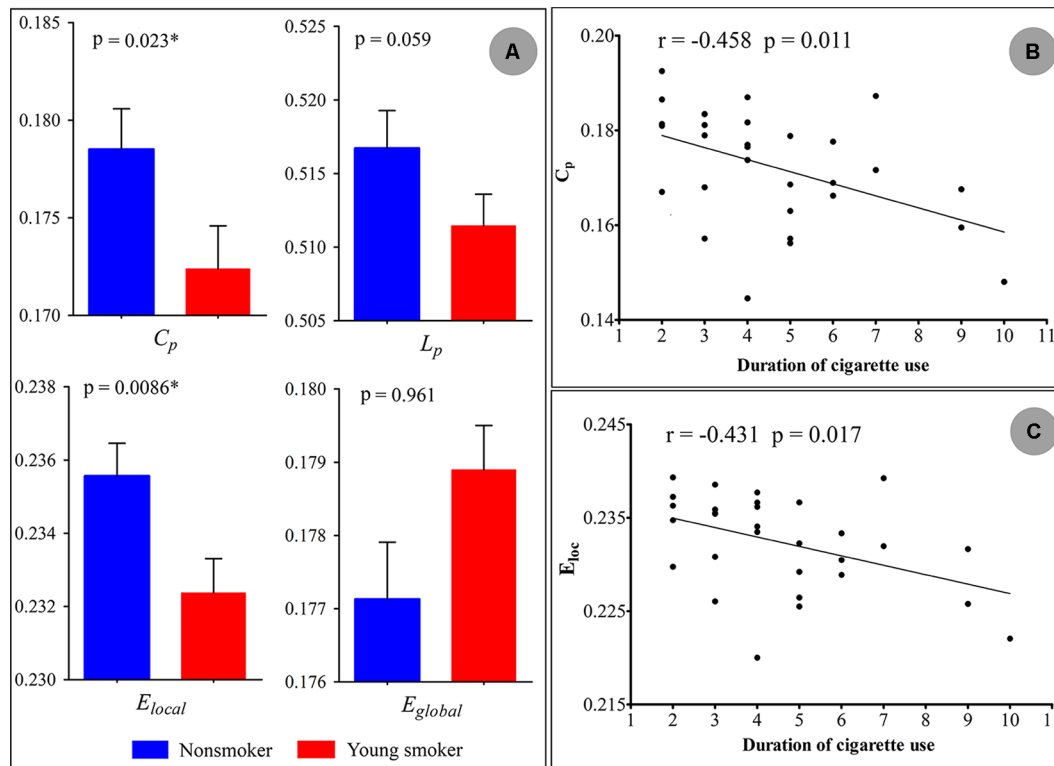


FIGURE 3 | (A) Statistical analysis revealed significant differences in the global parameters between the nonsmokers and young smokers. **(B and C)** The clustering coefficient (C_p ; $r = -0.458$; $p = 0.011$) and local network efficiency (E_{local} ; $r = -0.431$; $p = 0.017$) were negatively correlated with duration of cigarette use.

Nodal Characteristics of Brain Functional Networks

Compared to nonsmokers, young smokers exhibited significantly increased nodal efficiencies (E_{nodal}) in 10 regions ($p < 0.05$ after 5000 permutation tests; **Figure 4**): superior frontal gyrus: SFG_L_7_1 and SFG_R_7_1 (B/A, medial area 8), orbital gyrus: OrG_L_6_4 (B/A, medial area 11) and OrG_R_6_5 (B/A, area 11), precentral gyrus: PrG_L_6_1 (B/A, area 4) and PrG_R_6_5 (B/A, area 4), inferior parietal lobule: IPL_R_6_2 (B/A, rostradorsal area 39), insular gyrus: INS_R_6_3 (dorsal agranular insula), cingulate gyrus: CG_R_7_2 (B/A, rostroventral area 24), and basal ganglia: BG_R_6_1 (ventral caudate).

Abnormal Brain FC in Young Smokers

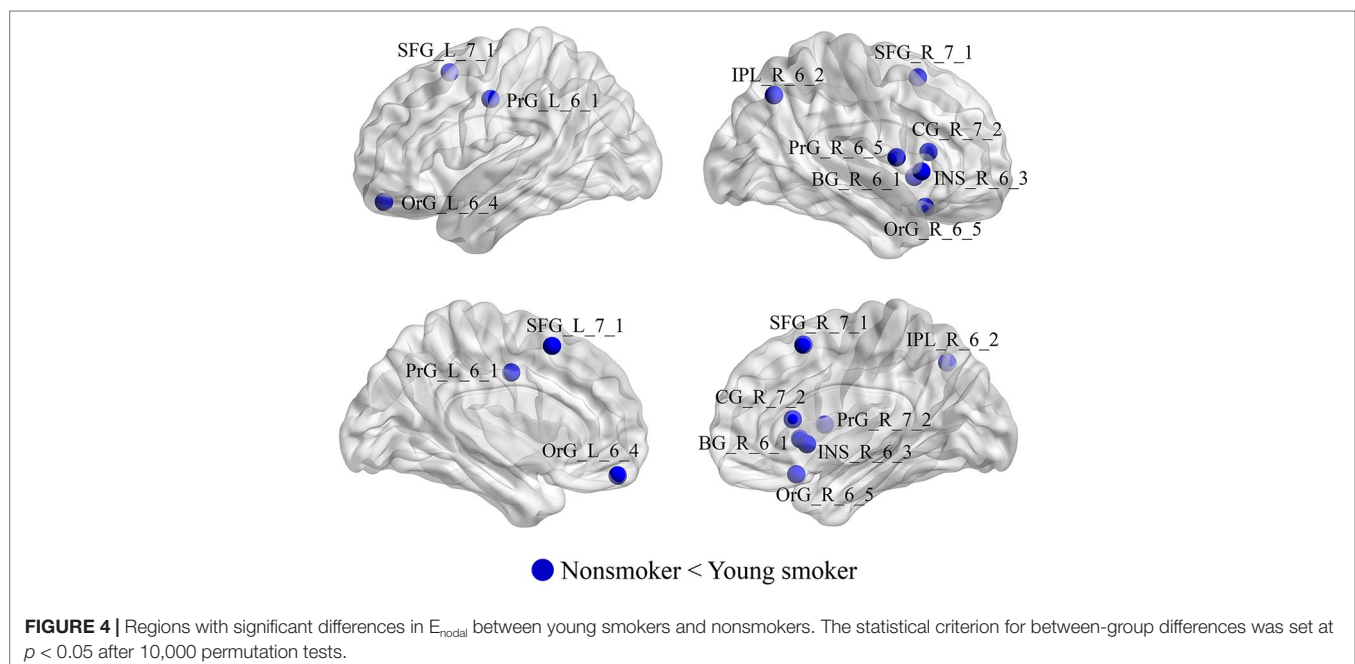
Compared to nonsmokers, young smokers showed increased connectivity, including 26 brain regions and 20 edges, such as the frontal lobe (superior frontal gyrus: SFG_R_7_2, middle frontal gyrus: MFG_L_7_6 and MFG_L_7_7, and inferior frontal gyrus: IFG_R_6_1), temporal lobe (middle temporal gyrus: MTG_L_4_3, inferior temporal gyrus: ITG_L_7_2 and ITG_R_7_2, and parahippocampal gyrus: PhG_R_6_3 and PhG_L_6_6), parietal lobe (inferior parietal lobule: IPL_L_6_1 and precuneus: PCun_R_4_4), insular lobe (insula: INS_L_6_1), limbic lobe (cingulate gyrus: CG_L_7_3, CG_L_7_4 and CG_R_7_4), occipital lobe (medioventral occipital cortex: MVOcC_R_5_2 and MVOcC_R_5_3 and lateral occipital cortex: LOcC_L_4_2), and subcortical nuclei (basal ganglia [BG]: BG_L_6_3, BG_R_6_3 and BG_R_6_4, thalamus: Tha_L_8_2, Tha_R_8_2, Tha_R_8_5, and Tha_R_8_8; **Figure 5A**). Moreover, the t values of statistical analyses in the connections between two groups are shown in **Figure 5B**.

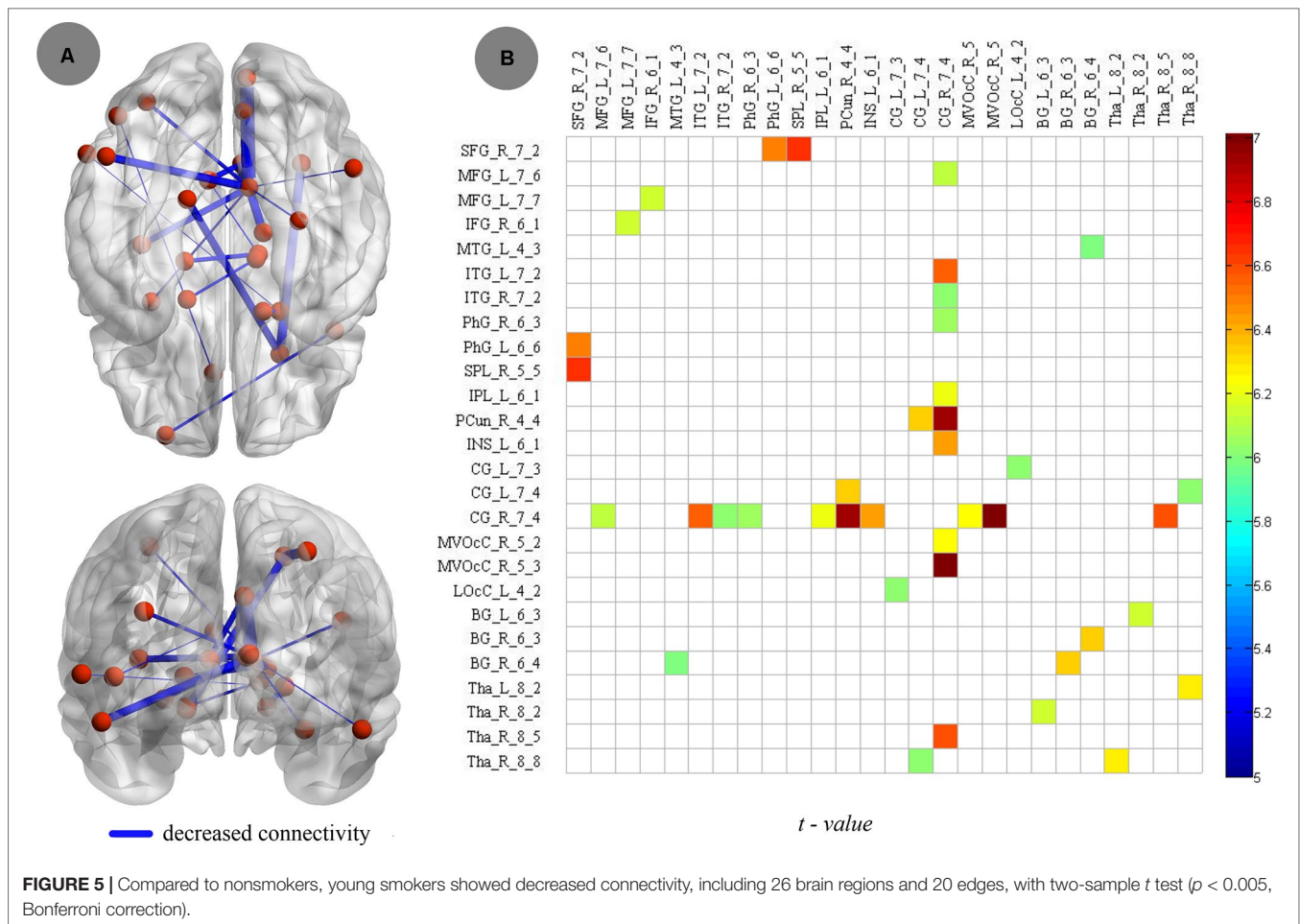
DISCUSSION

In this study, we investigated the topological organization of brain functional networks in nonsmokers and young smokers. The results are as follows: (1) At the global level, the topological organization of brain functional networks in the two groups consistently showed the small-world property, whereas the global topological organization differed significantly between nonsmokers and young smokers — young smokers showed a significantly decreased C_p and E_{local} . C_p and E_{local} were negatively correlated with the duration of cigarette use. (2) At the regional level, changes in nodal E_{global} were mainly found in the frontal gyrus, cingulate gyrus, insula, and BG. (3) At the connectivity level, increased connectivity in young smokers was primarily detected in the frontal gyrus, cingulate gyrus, BG, and thalamus. These findings may improve the understanding of neurophysiologic mechanisms in whole-brain functional networks in young smokers.

Global Parameters

The brain function networks in both nonsmokers and young smokers showed the small-world property. Small-world organization is one of the most influential findings about human brain functional networks and is a promising characteristic to describe large-scale brain networks. A small-world network has high local C_p and L_p (35) as well as highly effective local information processing and rapid global information transfer, which supports both specialized processing in local clusters and integrated processing over the entire network (25) and maintains an optimal balance between local specialization and global integration (36). Previous human brain functional network studies have identified the small-world property using various imaging techniques, such as magnetoencephalography, electroencephalography, and functional MRI (19, 22, 24, 37). Consistent with previous studies, in the current study, we observed





that both nonsmokers and young smokers showed small-world architecture in the brain functional networks (Figures 1 and 2).

Although a small-world topology was detected in both nonsmokers and young smokers’ brain functional networks, there were significant group differences in network global properties. Compared to nonsmokers, young smokers showed significantly decreased global parameters in C_p and E_{local} (Figure 3A). Moreover, C_p and E_{local} were negatively correlated with the duration of cigarette use (Figure 3B, C). C_p and E_{local} describe the concentrated clustering of local connections and measure local information transmission and processing capacity (38). In the current study, C_p and E_{local} were significantly decreased in young smokers, which revealed weaker local information processing capacity and more difficult information transfer with cliquishness in young smokers. Brain structural connectivity (SC) and FC are strongly related in network topologic organization. SC is the basis of FC and can constrain and shape FC patterns across both local and global scales (39). Previous structural network study revealed that E_{local} in young smokers was increased in the whole brain (18). The increased E_{local} in SC and the decreased E_{local} in FC are complementary to ensure the information transmission efficiency in young smokers.

A longer duration of cigarette use caused lower C_p and decreased E_{local} of brain networks. These findings suggest that the correlation is a consequence of the length of cigarette smoking

during adolescence. However, Lin et al. found contradictory effects of smoking on the brain function in global topological parameters, showing that chronic smokers had higher C_p and E_{local} compared to matched nonsmokers (25). The contradictory effects on the brain functional networks may be related subjects’ individual differences, smoking onset age, duration of cigarette use, age, and exposure time to nicotine in young smokers and chronic or heavy smokers. Further research is needed to confirm the validity of the results.

Nodal Parameters

We found that increased E_{nodal} in young smokers was primarily in the PFC [including superior frontal gyrus, orbital cortex (OFC), and precentral gyrus], cingulate cortex (B/A 24), dorsal insula, and ventral caudate compared to nonsmokers. Previous studies found that the PFC, cingulate cortex, and insula exhibited smoking-related abnormalities in gray matter morphology, such as reduced cortical thickness and gray matter volume and density (10, 40–45). The PFC is related to motivation and cognitive control in addiction (41, 46–48). Additionally, the OFC plays an important role in generating outcome expectancies that guide decision-making in reinforcement devaluation tasks, and the superior frontal gyrus is closely related to cognitive control (49–52). Previous studies showed that cingulate cortex activation is related to cigarette craving in smokers. The insula is connected with the OFC and

cingulate cortex (53–55). Moreover, previous studies mentioned that the insula was involved in the craving and showed significant smoking cue-elicited activation in smokers (44, 53, 56). In addition, mounting evidence suggests that the caudate plays a critical role in the craving of smokers, being significantly correlated with craving ratings (57, 58). In the current study, the increased efficiency in PFC, cingulate cortex, insular, and caudate in young smokers may increase the craving to smoke, thus making it difficult for young smokers to halt the development of nicotine dependence and uncontrollable compulsive drug-seeking behavior.

Connectivity

Neurobiological models of addiction posit that impaired communication between brain regions may contribute significantly to the behavioral deficits of smokers (18). In the current study, we observed the significantly abnormal connectivity in cortical (PFC, cingulate cortex, and insula) and subcortical (BG and thalamus) regions. The primary decreased connectivity was between the cingulate cortex and the PFC, insula, and thalamus. Previous studies found that cingulate cortex activity is associated with cognitive control (59, 60) and that changes in the activity of the cingulate cortex are correlated with the cognitive deficits in smokers (61). The insula is closely related to smoking behavior, such as cognitive control and craving (53). The activation of the insula was correlated with smokers' ratings of urge to smoke when they were exposed to smoking-related cues or deprived of smoking (62–64). In addition, abnormal SC between the cingulate cortex and insula was also detected and found to be related to impaired cognitive control in adolescents with Internet gaming disorder (65). Our previous studies demonstrated that the PFC plays a critical role in cognitive control deficits in young smokers (13, 66, 67). The decreased FC in cingulate, insula, and PFC found in the current study may demonstrate that the interaction between the two regions plays a critical role in the cognitive impairments of young smokers. We also found decreased FC in the subcortical region between the BG and thalamus. The BG is a part of the nigrostriatal dopamine circuit, which plays an important role in craving and reward processing in addiction (13, 67–69). In addition, in smoking studies, BG was found to mainly regulate the rewarding effect of smoking and motivation to smoke (57, 70). Previous research found that the thalamus is also related to the reward processing and cognitive control functions (71–74). Therefore, the reduced connectivity between the BG and thalamus in young smokers may provide more scientific evidence

for the cause of increased craving in young smokers. The main areas of decreased FC were the PFC, insula, cingulate cortex, BG, and thalamus, which are particularly implicated in the cognitive control, reward-seeking, motivation, and compulsive drug intake that have been put forward to explain the phenomenon of addiction.

The novelty of the current study was the choice of 246 regions to build the network. We replicated previous findings by revealing decreased C_p and E_{local} in smokers. In addition, we extended a previous study by demonstrating the RSFC among the PFC, caudate, thalamus, and insular in smokers in a higher spatial resolution. Due to the lack of cognitive tasks, the conclusions and hypotheses should be tested in the future. In the current study, we enrolled only male participants, which suggested that the results may only generalize to males. The cross-sectional experiment design cannot separate the results observed in the current study were the consequences or causes of smoking.

DATA AVAILABILITY

The datasets generated for this study are available on request to the corresponding author.

ETHICS STATEMENT

All of the procedures of the present study were approved by the Medical Ethical Committee of the Xiangya Hospital of Central South University. All of the participants and their parents gave the written informed consent after the experimental procedure was fully explained.

AUTHOR CONTRIBUTIONS

YT, WL, and ZQ conceived and designed the experiments. YT, WL, and JC conducted the experiments and collected data. YT analyzed the data. YT and WL wrote the paper.

FUNDING

This work was supported by research grants from the Scientific Research Project of Health and Family Planning Commission of Hunan Province, China (B2019179).

REFERENCES

- Glantz SA, Parmley WW. Passive smoking and heart disease. Epidemiology, physiology, and biochemistry. *Circulation* (1991) 83(1):1–12. doi: 10.1161/01.CIR.83.1.1
- Galván A, Poldrack RA, Baker CM, McClennen KM, London ED. Neural correlates of response inhibition and cigarette smoking in late adolescence. *Neuropsychopharmacology* (2011) 36(5):970–8. doi: 10.1038/npp.2010.235
- O'Loughlin J, DiFranza J, Tyndale RF, Meshfedjian G, McMillan-Davey E, Clarke PB, et al. Nicotine-dependence symptoms are associated with smoking frequency in adolescents. *Am J Prev Med* (2003) 25(3):219–25. doi: 10.1016/S0749-3797(03)00198-3
- Taioli E, Wynder EL. Effect of the age at which smoking begins on frequency of smoking in adulthood. *N Engl J Med* (1991) 325(13):968–9. doi: 10.1056/NEJM199109263251318
- White HR, Bray BC, Fleming CB, Catalano RF. Transitions into and out of light and intermittent smoking during emerging adulthood. *Nicotine Tob Res.* (2009) 11(2):211–9. doi: 10.1093/ntr/ntn017
- Yuan K, Yu D, Bi Y, Li Y, Guan Y, Liu J, et al. The implication of frontostriatal circuits in young smokers: a resting-state study. *Hum Brain Mapp* (2016) 37(6):2013–26. doi: 10.1002/hbm.23153
- Yuan K, Yu D, Bi Y, Wang R, Li M, Zhang Y, et al. The left dorsolateral prefrontal cortex and caudate pathway: new evidence for cue-induced craving of smokers. *Hum Brain Mapp* (2017) 38(9):4644–56. doi: 10.1002/hbm.23690

8. Yuan K, Yu D, Zhao M, Li M, Wang R, Li Y, et al. Abnormal frontostriatal tracts in young male tobacco smokers. *Neuroimage* (2018) 183:346–55. doi: 10.1016/j.neuroimage.2018.08.046
9. Yuan K, Zhao M, Yu D, Manza P, Volkow ND, Wang GJ, et al. Striato-cortical tracts predict 12-h abstinence-induced lapse in smokers. *Neuropsychopharmacology* (2018) 43(12):2452–8. doi: 10.1038/s41386-018-0182-x
10. Li Y, Yuan K, Cai C, Feng D, Yin J, Bi Y, et al. Reduced frontal cortical thickness and increased caudate volume within fronto-striatal circuits in young adult smokers. *Drug Alcohol Depend* (2015) 151:211–9. doi: 10.1016/j.drugalcdep.2015.03.023
11. Liao Y, Tang J, Deng Q, Deng Y, Luo T, Wang X, et al. Bilateral fronto-parietal integrity in young chronic cigarette smokers: a diffusion tensor imaging study. *PLoS One* (2011) 6(11):e26460. doi: 10.1371/journal.pone.0026460
12. Hong LE, Gu H, Yang Y, Ross TJ, Salmeron BJ, Buchholz B, et al. Association of nicotine addiction and nicotine's actions with separate cingulate cortex functional circuits. *Arch Gen Psychiatry* (2009) 66(4):431–41. doi: 10.1001/archgenpsychiatry.2009.2
13. Feng D, Yuan K, Li Y, Cai C, Yin J, Bi Y, et al. Intra-regional and inter-regional abnormalities and cognitive control deficits in young adult smokers. *Brain Imaging Behav* (2016) 10(2):506–16. doi: 10.1007/s11682-015-9427-z
14. Chu S, Xiao D, Wang S, Peng P, Xie T, He Y, et al. Spontaneous brain activity in chronic smokers revealed by fractional amplitude of low frequency fluctuation analysis: a resting state functional magnetic resonance imaging study. *Chin Med J (Engl)* (2014) 127(8):1504–9.
15. Yu R, Zhao L, Tian J, Qin W, Wang W, Yuan K, et al. Regional homogeneity changes in heavy male smokers: a resting-state functional magnetic resonance imaging study. *Addict Biol* (2013) 18(4):729–31. doi: 10.1111/j.1369-1600.2011.00359.x
16. Liao X, Vasilakos AV, He Y. Small-world human brain networks: perspectives and challenges. *Neurosci Biobehav Rev* (2017) 77:286–300. doi: 10.1016/j.neubiorev.2017.03.018
17. Yuan K, Qin W, Liu J, Guo Q, Dong M, Sun J. Altered small-world brain functional networks and duration of heroin use in male abstinent heroin-dependent individuals. *Neurosci Lett* (2010) 477(1):37–42. doi: 10.1016/j.neulet.2010.04.032
18. Zhang Y, Li M, Wang R, Bi Y, Li Y, Yi Z, et al. Abnormal brain white matter network in young smokers: a graph theory analysis study. *Brain Imaging Behav* (2018) 12(2):345–56. doi: 10.1007/s11682-017-9699-6
19. Stam CJ, Reijneveld JC. Graph theoretical analysis of complex networks in the brain. *Nonlinear Biomed Phys* (2007) 1(1):3. doi: 10.1186/1753-4631-1-3
20. He Y, Evans A. Graph theoretical modeling of brain connectivity. *Curr Opin Neurol* (2010) 23(4):341–50. doi: 10.1097/WCO.0b013e32833aa567
21. Hong SB, Zalesky A, Cocchi L, Fornito A, Choi EJ, Kim HH, et al. Decreased functional brain connectivity in adolescents with internet addiction. *PLoS One* (2013) 8(2):e57831. doi: 10.1371/journal.pone.0057831
22. Jiang G, Wen X, Qiu Y, Zhang R, Wang J, Li M, et al. Disrupted topological organization in whole-brain functional networks of heroin-dependent individuals: a resting-state fMRI study. *PLoS One* (2013) 8(12):e82715. doi: 10.1371/journal.pone.0082715
23. Sun Y, Wang GB, Lin QX, Lu L, Shu N, Meng SQ, et al. Disrupted white matter structural connectivity in heroin abusers. *Addict Biol* (2017) 22(1):184–95. doi: 10.1111/adb.12285
24. Tschernegg M, Crone JS, Eigenberger T, Schwartenbeck P, Fauth-Bühler M, Leménager T, et al. Abnormalities of functional brain networks in pathological gambling: a graph-theoretical approach. *Front Hum Neurosci* (2013) 7:625. doi: 10.3389/fnhum.2013.00625
25. Lin F, Wu G, Zhu L, Lei H. Altered brain functional networks in heavy smokers. *Addict Bio* (2015) 20(4):809–19. doi: 10.1111/adb.12155
26. Cheng H, Wang Y, Sheng J, Sporns O, Kronenberger WG, Mathews VP, et al. Optimization of seed density in DTI tractography for structural networks. *J Neurosci Methods* (2012) 203(1):264–72. doi: 10.1016/j.jneumeth.2011.09.021
27. Wylie KP, Rojas DC, Tanabe J, Martin LE, Tregellas JR. Nicotine increases brain functional network efficiency. *Neuroimage* (2012) 63(1):73–80. doi: 10.1016/j.neuroimage.2012.06.079
28. Fan L, Li H, Zhuo J, Zhang Y, Wang J, Chen L, et al. The human brainnetome atlas: a new brain atlas based on connectonal architecture. *Cereb Cortex* (2016) 26(8):3508–26. doi: 10.1093/cercor/bhw157
29. Rudie JD, Brown JA, Beck-Pancer D, Hernandez LM, Dennis EL, Thompson PM, et al. Altered functional and structural brain network organization in autism. *Neuroimage Clin* (2012) 2:79–94. doi: 10.1016/j.nicl.2012.11.006
30. Achard S, Bullmore E. Efficiency and cost of economical brain functional networks. *PLoS Comput Biol* (2007) 3(2):e17. doi: 10.1371/journal.pcbi.0030017
31. Watts DJ, Strogatz SH. Collective dynamics of 'small-world' networks. *Nature* (1998) 393(6684):440–2. doi: 10.1038/30918
32. Maslov S, Sneppen K. Specificity and stability in topology of protein networks. *Science* (2002) 296(5569):910–3. doi: 10.1126/science.1065103
33. Humphries MD, Gurney K, Prescott TJ. Is there an integrative center in the vertebrate brain-stem? A robotic evaluation of a model of the reticular formation viewed as an action selection device. *Adaptive Behavior* (2005) 13(2):97–113. doi: 10.1177/105971230501300203
34. Latora V, Marchiori M. Efficient behavior of small-world networks. *Phys Rev Lett* (2001) 87(19):198701. doi: 10.1103/PhysRevLett.87.198701
35. Rubinov M, Sporns O. Complex network measures of brain connectivity: uses and interpretations. *Neuroimage* (2010) 52(3):1059–69. doi: 10.1016/j.neuroimage.2009.10.003
36. Sporns O. The human connectome: a complex network. *Ann N Y Acad Sci* (2011) 1224:109–25. doi: 10.1111/j.1749-6632.2010.05888.x
37. Bartolomei F, Bosma I, Klein M, Baayen JC, Reijneveld JC, Postma TJ, et al. Disturbed functional connectivity in brain tumour patients: evaluation by graph analysis of synchronization matrices. *Clin Neurophysiol* (2006) 117(9):2039–49. doi: 10.1016/j.clinph.2006.05.018
38. Fornito A, Zalesky A, Bullmore E. *Fundamentals of brain network analysis*. Salt Lake City of American: Academic Press (2016).
39. Wang Z, Dai Z, Gong G, Zhou C, He Y. Understanding structural-functional relationships in the human brain: a large-scale network perspective. *Neuroscientist* (2015) 21(3):290–305. doi: 10.1177/1073858414537560
40. Almeida OP, Garrido GJ, Lautenschlager NT, Hulse GK, Jamrozik K, Flicker L. Smoking is associated with reduced cortical regional gray matter density in brain regions associated with incipient Alzheimer disease. *Am J Geriatr Psychiatry* (2008) 16(1):92–8. doi: 10.1097/JGP.0b013e318157cad2
41. Brody AL, Mandelkern MA, Jarvik ME, Lee GS, Smith EC, Huang JC, et al. Differences between smokers and nonsmokers in regional gray matter volumes and densities. *Biol Psychiatry* (2004) 55(1):77–84. doi: 10.1016/S0006-3223(03)00610-3
42. Fritz HC, Wittfeld K, Schmidt CO, Domin M, Grabe HJ, Hegenscheid K, et al. Current smoking and reduced gray matter volume—a voxel-based morphometry study. *Neuropsychopharmacology* (2014) 39(11):2594–600. doi: 10.1038/npp.2014.112
43. Liao Y, Tang J, Liu T, Chen X, Hao W. Differences between smokers and non-smokers in regional gray matter volumes: a voxel-based morphometry study. *Addict Biol* (2012) 17(6):977–80. doi: 10.1111/j.1369-1600.2010.00250.x
44. Zhang J, Wang J, Wu Q, Kuang W, Huang X, He Y, et al. Disrupted brain connectivity networks in drug-naive, first-episode major depressive disorder. *Biol Psychiatry* (2011) 70(4):334–42. doi: 10.1016/j.biopsych.2011.05.018
45. Zhang X, Salmeron BJ, Ross TJ, Gu H, Geng X, Yang Y, et al. Anatomical differences and network characteristics underlying smoking cue reactivity. *Neuroimage* (2011) 54(1):131–41. doi: 10.1016/j.neuroimage.2010.07.063
46. Baler RD, Volkow ND. Drug addiction: the neurobiology of disrupted self-control. *Trends Mol Med* (2006) 12(12):559–66. doi: 10.1016/j.molmed.2006.10.005
47. Yuan F, Kong L, Zhu X, Jiang C, Fang C, Liao W. Altered gray-matter volumes associated with betel quid dependence. *Front Psychiatry* (2017) 8:139. doi: 10.3389/fpsy.2017.00139
48. Zhu X, Liu S, Liao W, Kong L, Jiang C, Yuan F. Executive function deficit in betel-quid-dependent chewers: mediating role of prefrontal cortical thickness. *J Psychopharmacol* (2018) 32:1362–8. doi: 10.1177/0269881118806299
49. Schoenbaum G, Roesch MR, Stalnaker TA. Orbitofrontal cortex, decision-making and drug addiction. *Trends Neurosci* (2006) 29(2):116–24. doi: 10.1016/j.tins.2005.12.006

50. Yuan K, Qin W, Yu D, Bi Y, Xing L, Jin C, et al. Core brain networks interactions and cognitive control in internet gaming disorder individuals in late adolescence/early adulthood. *Brain Struct Funct* (2016) 221(3):1427–42. doi: 10.1007/s00429-014-0982-7
51. Fan J, Zhong M, Zhu X, Gan J, Liu W, Niu C, et al. Resting-state functional connectivity between right anterior insula and right orbital frontal cortex correlate with insight level in obsessive-compulsive disorder. *Neuroimage Clin* (2017) 15:1–7. doi: 10.1016/j.nicl.2017.04.002
52. Zhu X, Zhu Q, Shen H, Liao W, Yuan F. Rumination and default mode network subsystems connectivity in first-episode, drug-naive young patients with major depressive disorder. *Sci. Rep.* (2017b) 7:43105. doi: 10.1038/srep43105
53. Bi Y, Yuan K, Guan Y, Cheng J, Zhang Y, Li Y, et al. Altered resting state functional connectivity of anterior insula in young smokers. *Brain imaging and behavior* (2016) 11(1):155–65. doi: 10.1007/s11682-016-9511-z
54. Deen B, Pitskel NB, Pelphrey KA. Three systems of insular functional connectivity identified with cluster analysis. *Cereb Cortex* (2011) 21(7):1498–506. doi: 10.1093/cercor/bhq186
55. Lu S, Xu R, Cao J, Yin Y, Gao W, Wang D, et al. The left dorsolateral prefrontal cortex volume is reduced in adults reporting childhood trauma independent of depression diagnosis. *J Psychiatr Res* (2019) 112:12–7. doi: 10.1016/j.jpsychires.2019.02.014
56. Janes AC, Nickerson LD, Frederick Bde B, Kaufman MJ. Prefrontal and limbic resting state brain network functional connectivity differs between nicotine-dependent smokers and non-smoking controls. *Drug Alcohol Depend* (2012) 125(3):252–9. doi: 10.1016/j.drugalcdep.2012.02.020
57. Barrett SP, Boileau I, Okker J, Pihl RO, Dagher A. The hedonic response to cigarette smoking is proportional to dopamine release in the human striatum as measured by positron emission tomography and [11C] raclopride. *Synapse* (2004) 54(2):65–71. doi: 10.1002/syn.20066
58. Brody AL, Olmstead RE, London ED, Farahi J, Meyer JH, Grossman P. Smoking-induced ventral striatum dopamine release. *Am J Psychiatry* (2004) 161(7):211–8. doi: 10.1176/appi.ajp.161.7.1211
59. Kerns JG, Cohen JD, MacDonald AW, 3rd, RY Cho, VA Stenger, Carter CS. Anterior cingulate conflict monitoring and adjustments in control. *Science* (2004) 303(5660):1023–6. doi: 10.1126/science.1089910
60. MacDonald AW, 3rd, Cohen JD, Stenger VA, Carter CS. Dissociating the role of the dorsolateral prefrontal and anterior cingulate cortex in cognitive control. *Science* (2000) 288(5472):1835–8. doi: 10.1126/science.288.5472.1835
61. Azizian A, Nestor LJ, Payer D, Monterosso JR, Brody AL, London ED. Smoking reduces conflict-related anterior cingulate activity in abstinent cigarette smokers performing a Stroop task. *Neuropsychopharmacology* (2010) 35(3):775–82. doi: 10.1038/npp.2009.186
62. Brody AL, Mandelkern MA, Olmstead RE, Jou J, Tjongson E, Allen V. Neural substrates of resisting craving during cigarette cue exposure. *Biol Psychiatry* (2007) 62(6):642–51. doi: 10.1016/j.biopsych.2006.10.026
63. Engelmann JM, Versace F, Robinson JD, Minnix JA, Lam CY, Cui Y. Neural substrates of smoking cue reactivity: a meta-analysis of fMRI studies. *Neuroimage* (2012) 60(1):252–62. doi: 10.1016/j.neuroimage.2011.12.024
64. Moran-Santa Maria MM, Hartwell KJ, Hanlon CA, Canterberry M, Lematty T, Owens M, et al. Right anterior insula connectivity is important for cue-induced craving in nicotine-dependent smokers. *Addict Biol* (2015) 20(2):407–14. doi: 10.1111/adb.12124
65. Xing L, Yuan K, Bi Y, Yin J, Cai C, Feng D, et al. Reduced fiber integrity and cognitive control in adolescents with internet gaming disorder. *Brain Res* (2014) 1586:109–17. doi: 10.1016/j.brainres.2014.08.044
66. Yin J, Yuan K, Feng D, Cheng J, Li Y, Cai C, et al. Inhibition control impairments in adolescent smokers: electrophysiological evidence from a Go/NoGo study. *Brain Imaging Behav* (2016) 10(2):497–505. doi: 10.1007/s11682-015-9418-0
67. Yuan K, Yu D, Cai C, Feng D, Li Y, Bi Y, et al. Frontostriatal circuits, resting state functional connectivity and cognitive control in internet gaming disorder. *Addict Biol* (2017) 22(3):813–22. doi: 10.1111/adb.12348
68. Delgado MR, Nystrom LE, Fissell C, Noll DC, Fiez JA. Tracking the hemodynamic responses to reward and punishment in the striatum. *J Neurophysiol* (2000) 84(6):3072–7. doi: 10.1152/jn.2000.84.6.3072
69. Volkow ND, Wang GJ, Telang F, Fowler JS, Logan J, Childress AR, et al. Cocaine cues and dopamine in dorsal striatum: mechanism of craving in cocaine addiction. *J Neurosci* (2006) 26(24):6583–8. doi: 10.1523/JNEUROSCI.1544-06.2006
70. Le Foll B, Guranda M, Wilson AA, Houle S, Rusjan PM, Wing VC, et al. Elevation of dopamine induced by cigarette smoking: novel insights from a [11C]-+PHNO PET study in humans. *Neuropsychopharmacology* (2014) 39(2):415–24. doi: 10.1038/npp.2013.209
71. Corbit LH, Muir JL, Balleine BW. Lesions of mediodorsal thalamus and anterior thalamic nuclei produce dissociable effects on instrumental conditioning in rats. *Eur J Neurosci* (2003) 18(5):1286–94. doi: 10.1046/j.1460-9568.2003.02833.x
72. Rieck RW, Ansari MS, Whetsell WO Jr, Deutch AY, Kessler RM. Distribution of dopamine D2-like receptors in the human thalamus: autoradiographic and PET studies. *Neuropsychopharmacology* (2004) 29(2):362–72. doi: 10.1038/sj.npp.1300336
73. Yu C, Gupta J, Yin HH. The role of mediodorsal thalamus in temporal differentiation of reward-guided actions. *Front Integr Neurosci* (2010) 4:14. doi: 10.3389/fnint.2010.00014
74. Yu D, Yuan K, Cheng J, Guan Y, Li Y, Bi Y, et al. Reduced thalamus volume may reflect nicotine severity in young male smokers. *Nicotine Tob Res* (2018) 20(4):434–9. doi: 10.1093/ntr/ntx146

Conflict of Interest Statement: The authors declare that the research was conducted in the absence of any commercial or financial relationships that could be construed as a potential conflict of interest.

Copyright © 2019 Tan, Chen, Liao and Qian. This is an open-access article distributed under the terms of the Creative Commons Attribution License (CC BY). The use, distribution or reproduction in other forums is permitted, provided the original author(s) and the copyright owner(s) are credited and that the original publication in this journal is cited, in accordance with accepted academic practice. No use, distribution or reproduction is permitted which does not comply with these terms.